Yu *et al. Applied Biological Chemistry* (2022) 65:51
https://doi.org/10.1186/s13765-022-00721-x

KSABC
The Korean Society for Applied Biological Chemistry

ARTICLE Open Access

An electrochemical sensor based on $[Ru(bpy)_2dpp]^{2+}$/SMWCNTs/Au modified glassy carbon electrode for the detection of 5′-GMP

Ying Yu[1], Siqi Huan[1], Xiaodan Wang[3], Cong Yang[1] and Dengyong Liu[1,2*]

Abstract

A sensitive electrochemical sensor for the selective detection of 5′-guanylic acid (5′-GMP) was prepared by combining sulfonated-multiwalled carbon nanotubes (SMWCNTs) and $[Ru(bpy)_2dpp]Cl_2$, which were dripped on the surface of a glass carbon electrode (GCE) immobilized with gold nanoparticles. The 5′-GMP electrochemical biosensor was fabricated using $[Ru(bpy)_2dpp]^{2+}$/SMWCNTs/Au/GCE as working, Ag/AgCl as reference and Pt as auxiliary electrode connected by an electrochemical workstation. The modified electrode was characterized by cyclic voltammetry (CV) and electrochemical impedance spectroscopy (EIS). The results showed the sensor's response current had the best peak shape and maximum peak when the pH of electrolyte was 3, scan speed of CV was in the range of 100 to 180 mV/s, and the enrichment time was in the range of 200 to 300 s. Under the optimum conditions, a linear analytical curve was obtained for 5′-GMP concentrations in the range of 0.01 to 0.5 mmol L^{-1}, with a detection limit of 0.0014 mmol L^{-1}. The analytical results of the 5′-GMP sensor were exhibited good consistent with the data from liquid chromatography. The sensor has good reproducibility, long-term stability and strong immunity to interference, and may be a powerful device for 5′-GMP detection, with great advantages such as simple preparation and operation, low equipment cost.

Keywords: 5′-Guanosine monophosphate, Polypyridyl ruthenium (II) complexes, Electrochemical sensor, Quantitative detection

Introduction

The umami taste of broth is an important index to evaluate the quality of actual products. The important taste substances in the soup include amino acids and nucleotides, among which inosinic acid and guanosinic acid in nucleotides are important umami flavoring substances, which can give the broth a delicious taste. 5′-GMP as one of the main sources of umami that is widely distributed in foods, especially in broths, braised brines and meat products, and is also a common food additive in food processing [1, 2]. 5′-GMP consists of ribose, phosphate and guanine. It has a fresh taste and can act synergistically with glutamate to greatly improve the flavor of food [3]. As a representative nucleotide for umami, 5′-GMP plays an important role in the overall flavor of foods, but it is difficult to detect by convenient techniques. Therefore, there is a need to establish a simple, accurate, and efficient method to detect and analyze 5′-GMP in food products.

So far, the techniques used to detect 5′-GMP are mainly ion chromatography, capillary electrophoresis and

*Correspondence: jz_dyliu@126.com

[1] National and Local Joint Engineering Research Center of Storage,, Processing and Safety Control Technology for Fresh Agricultural and Aquatic Products, College of Food Science and Technology, Bohai University, Jinzhou 121013, China
Full list of author information is available at the end of the article

high-performance liquid chromatography [4–6]. Compared with traditional instrumental analytical techniques, electrochemical techniques offer attractive advantages such as higher sensitivity, faster response time, simpler instrumentation, and easier on-line detection without complicated pretreatment, expensive equipment, skilled personnel, and long analysis times. In recent years, electrochemical detection methods have been widely used for the detection and analysis of pesticides, amino acids, heavy metals and other chemical substances [7–10].

$[Ru(bpy)_2dpp]Cl_2$ is a polypyridyl ruthenium (II) complex with unique photophysical activity and excellent electrochemical properties [11]. Has been widely used in DNA structural probes, molecular optical switches and anti-cancer drugs [12, 13]. The ligand of dpp in $[Ru(bpy)_2dpp]Cl_2$ contains two uncoordinated N atoms and thus can be firmly attached to the surface of the glassy carbon electrode. $[Ru(bpy)_2dpp]Cl_2$ are excellent mediators for catalytic oxidation of guanine. 5′-GMP oxidation is related to the sensitive substance and catalytically active compound of the modified electrode, and SMWCNTs can be effectively oxidized in the presence of polypyridyl ruthenium (II) complexes [14–17].

In this work, we constructed the $[Ru(bpy)_2dpp]^2+$/SMWCNTs/Au/GCE sensor by coating Au/GCE with a coating made from a mixture of SMWCNT and $[Ru(bpy)_2dpp]Cl_2$. The electrochemical behavior of its detection of 5′-GMP was characterized as well as the optimization of the effective experimental variables on the modified electrode. The experimental results demonstrate that the method is applicable to liquid samples with high accuracy and reliability and has potential applications for food quality control.

Experimental

Reagents and apparatus

Cis-Bis (2,2′-bipyridine) dichlororuthenium (II) hydrate (≥ 99.0%), SMWCNTs (2–5 nm of inner diameter, 10–30 μm of length), and N, N-Dimethylformamide (99.8%, DMF) were from Sigma-Aldrich Co. Ltd. (America). The standard substances such as 5′-GMP, L-glutamic acid (L-Glu), aspartic acid (Asp), inosine 5′-monophosphate (5′-IMP), and adenosine 5′-monophosphate (5′-AMP) were from Shanghai Aladdin Co. Ltd. (Shanghai, China). The phosphate buffer solutions (PBS) were prepared by $Na_2HPO_4{\cdot}12H_2O$ (AR) and $C_6H_8O_7{\cdot}H_2O$ (AR). Solutions of 5′-GMP were prepared in PBS. Other chemical reagents are analytical grade pure reagents on the market.

Apparatus and measurements

All electrochemical experiments and electrochemical impedance spectroscopic studies were carried out by CHI660E Electrochemical Workstation from Shanghai CH Co. Ltd. (Shanghai, China). Electrochemical measurements were performed using a conventional three-electrode system consisting of KCl-saturated Ag/AgCl as the reference electrode, Pt wire as the counter electrode and a modified GCE of 3 mm diameters as the working electrode. Separation was performed using a high-performance liquid chromatograph (HPLC) (Agilent 1260, USA) with a binary mobile phase and a column (Tosoh ODS-80TM, Japan) with gradient elution.

Construction of $[Ru(bpy)_2dpp]^{2+}$/SMWCNTs/Au/GCE modified electrode

To prepare $[Ru(bpy)_2dpp]^{2+}$/SMWCNTs/Au/GCE, the GCE surface was polished with 1 μm, 0.3 μm, and 0.05 μm alumina slurries on a polishing cloth to prior to immobilization. The polished electrodes were cleaned in ethanol (75%) to remove adsorbed particles and then activated in a solution of 0.5 mol L^{-1} H_2SO_4 using the CV method. During activation, the potential range was -1 to 1 V and the scan rate was 100 mV s^{-1}. The activation of the electrode was carried out until a stable and reproducible CV curve appeared [18]. After activation, the electrode was removed, rinsed with deionized water and blown dry with N_2 gas.

The pretreated bare GCE was scanned in 5 mmol L^{-1} chloroauric acid solution using the CV method. Parameters were set as follows: the scan potential range was -0.2 to 0.5 V, the scan rate was 50 mV s^{-1}, and the scan segments was 20. Removed the GCE and rinsed repeatedly with deionized water. The electrode of Au/GCE was obtained until its surface appeared rose-red [19].

The preparation of $[Ru(bpy)_2dpp]Cl_2$ was known as Bhuiyan's method [20]. 0.2 mmol of 4,7-diphenyl-1,10-phenanthroline and 0.2 mmol of $Ru(bpy)_2Cl_2$ were dissolved in 30 mL of aqueous 75% ethanol. The mixed solution was heated to reflux at 85 ℃ for 0.5 h, cooled to room temperature, and then mixed with the 100 to 200 mesh pure silica gel powder. The solvent of the mixture was evaporated by rotary evaporator at 85 ℃ until the blood-red silica gel powder was obtained. The silica gel powder with the color of blood-red color was extracted by chromatography. After further separation and purification, orange $[Ru(bpy)_2dpp]Cl_2$ solid was obtained.

DMF was used as a dispersant to dissolve $[Ru(bpy)_2dpp]Cl_2$ and SMWCNTs in a mass ratio of 4:25. 10 μL of the mixed solution was dropped on the surface of Au/GCE to make an electrode of $[Ru(bpy)_2dpp]^{2+}$/SMWCNTs/Au/GCE.

Testing and optimization of electrochemical sensor

To test the electrochemical sensor, experimental conditions such as the immobilization method of gold

nanoparticles, pH of electrolyte, CV scan rate and enrichment time were optimized using a completely randomized design approach.

The CV method was used to detect 5′-GMP with the following parameter settings: E_{init} was 0.6 V, E_{high} was 1.5 V, E_{low} was 0.6 V, E_{final} was 1.5 V, initial scan polarity was positive, scan rate was 100 mV s^{-1}, sensitivity was 1.0×10^{-4} A and scan segments was 4. Simultaneously, the preconditioned potential and time were set to 0.6 V and 300 s, respectively. The content of 5′-GMP in the sample was determined by substitution method. Electrochemical impedance spectroscopy tests were conducted at steady-state potentials.

CV data were analyzed by Origin software. The 5′-GMP oxidation peak current values were collected and linearly fitted to observe the different responses of the 5′-GMP sensor to different solutions. Finally, the CV plots and the fitted plots were combined into one image for a more visual observation.

Determination of 5′-GMP in broth by electrochemical sensor

The broth sample was provided by Shandong Dezhou Braised Chicken Co., LTD. The sauce marinated broth used for the actual sample assay was obtained from three different cooking pots. The broth was filtered through 200 mesh gauze and centrifuged with ethyl acetate (V: V = 1:1) at 10,000 r/min for 10 min at 4 °C. The supernatant was collected and adjusted to pH = 3 with HCl. All measurements were repeated three times at room temperature of 25 °C. To determine the 5′-GMP in the sauce marinated broth, the same procedure as for sensor response measurements was used under optimal working conditions.

Results

Surface characterization of modified electrodes

The morphology of Au NPs, SMWCNTs and Au NPs/SMWCNTs was characterized by SEM technique. In Fig. 1A, the SEM images show that each Au NPs had a

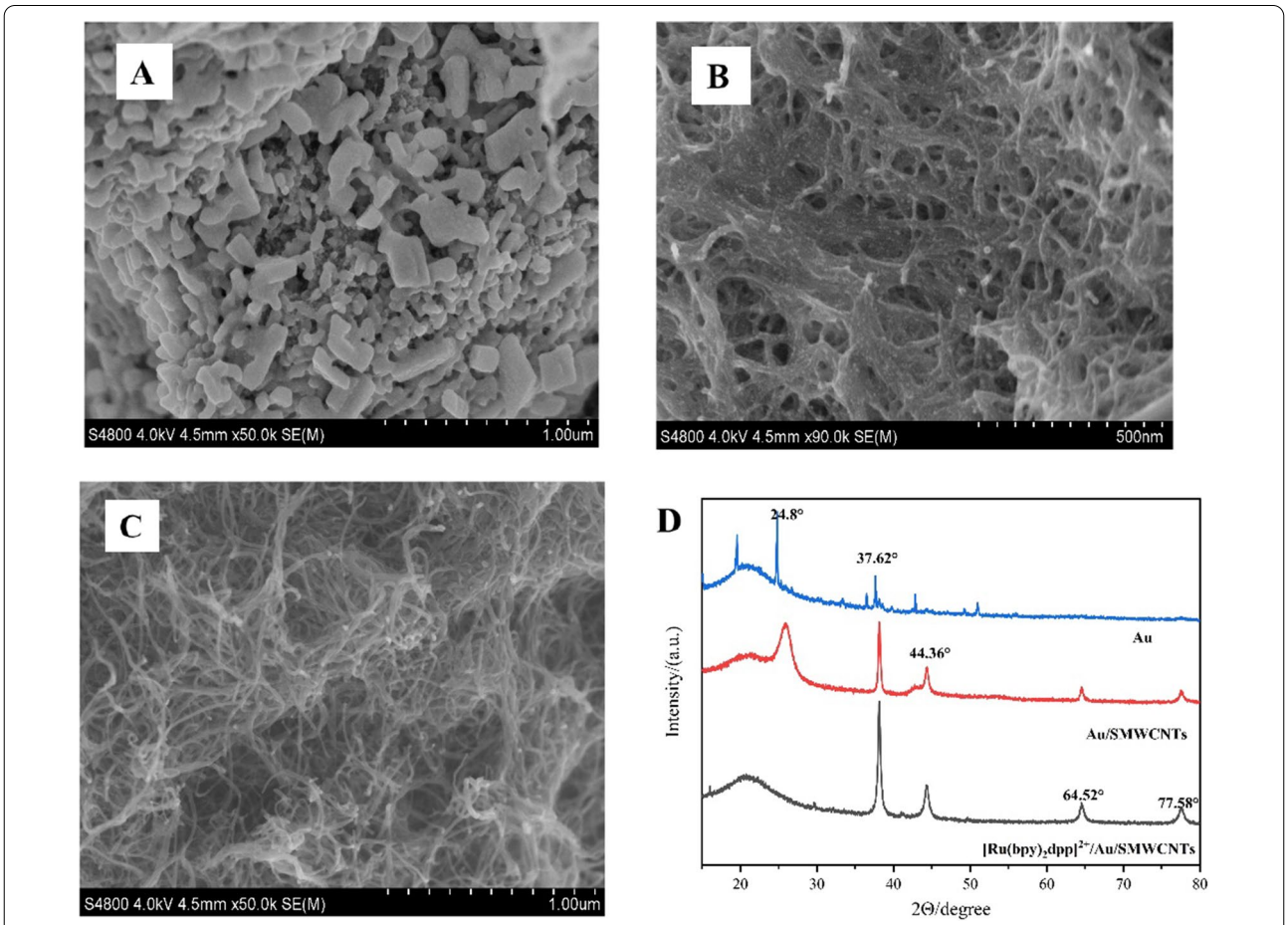

Fig. 1 SEM images obtained for **A** Au NPs, **B** SMWCNTs powder and **C** Au NPs/SMWCNTs. **D** XRD patterns of $[Ru(bpy)_2dpp]^{2+}$/SMWCNTs/Au

three-dimensional structure and well-distributed state, which not only maintains its large specific surface area and structural advantages, but also has good electrical properties [21]. Figure 1B shows the SEM images obtained for SMWCNTs powder that were entangled and interconnected in a mesh-like porous structure [22]. And as presented in Fig. 1C, a lot of Au NPs are tightly and dispersedly decorated on the SMWCNTs surface without aggregation status, which clearly indicates that Au NPs/SMWCNTs nanocomposite have been obtained and can be a good platform for sensing applications [23]. Figure 1D showed the XRD patterns for Au, Au/SMWCNTs and $[Ru(bpy)_2dpp]^{2+}$/SMWCNTs/Au. The XRD of Au exhibited diffraction peak at 24.8°and 37.62°, and a new peak of Au/SMWCNTs weas observed at 44.36°. The peak at 24.8 was assigned and enhanced the 64.52 and 77.58 diffraction peak in $[Ru(bpy)_2dpp]^{2+}$/SMWCNTs/Au. The results imply that the successful introduction of the Au/SMWCNTs and the synthesis of $[Ru(bpy)_2dpp]^{2+}$/SMWCNTs/Au nanocomposite.

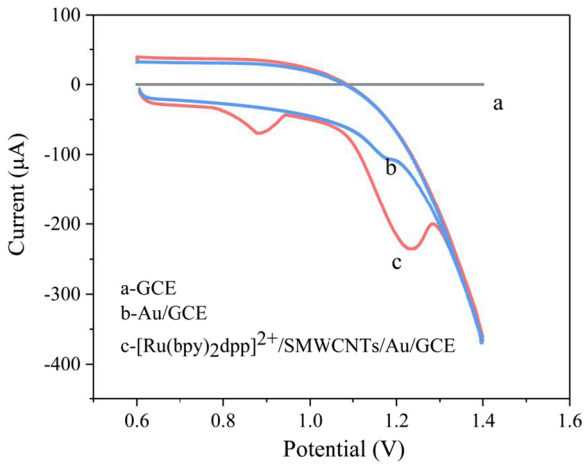

Fig. 2 CV curves of GCE, Au/GCE, and $[Ru(bpy)_2dpp]^{2+}$/SMWCNTs/Au/GCE in the solution of 0.1 mmol L^{-1} 5′-GMP. Parameters: $v = 100$ mV s^{-1}, E_{range} = from 0.6 to 1.5 V, the sensitivity was $1e^{-4}$ A, and the sweep segments were 4. Simultaneously, the precondition potential and time was set to 0.6 V, 300 s, respectively

CV and EIS characterizations of modified electrodes

CV measurements were performed to assess the electrochemical behavior of $[Ru(bpy)_2dpp]^{2+}$/SMWCNTs/Au/GCE on 5′-GMP solutions. The voltametric behavior of bare GCE, Au/GCE and $[Ru(bpy)_2dpp]^{2+}$/SMWCNTs/Au/GCE in the absence of 0.1 mmol L^{-1} 5′-GMP is shown in Fig. 2. As shown in Fig. 2, these three CV curves were obtained from three parallel experimental studies with deviation values of the upper and lower oxidation peak currents ranging from 0 to 11 μA. The response current of bare GCE in the presence of 5′-GMP was 0 V. The response current of Au/GCE showed a weak oxidation peak corresponding to the oxidation reaction of 5′-GMP with a peak potential of 1.2 V. The response current of $[Ru(bpy)_2dpp]^{2+}$/SMWCNTs/Au/GCE exhibited two well-characteristic oxidation peaks with peak potentials of 0.85 V and 1.25 V, respectively. The oxidation peak at 0.85 V corresponded to the reaction of $[Ru(bpy)_2dpp]^{2+} \rightarrow [Ru(bpy)_2dpp]^{3+} + e^-$ and the oxidation peak at 1.25 V corresponded to the reaction of $[Ru(bpy)_2dpp]^{3+}$ + 5′-GMP $\rightarrow [Ru(bpy)_2dpp]^{2+}$ + 5′-GMP_{OX}. The appearance of each oxidation peak in the figure was consistent with the 5′-GMP oxidation law [24]. Previous studies have shown that 5′-GMP is most likely to be oxidized in four nucleotides (adenine nucleotides, guanylate, cytidylate, and thymidine-5′-monophosphoric) [25, 26]. In addition, $[Ru(bpy)_2dpp]^{2+}$ could efficiently and specifically oxidize 5′-GMP in the presence of SMWCNTs [27]. The electrocatalytic kinetics of $[Ru(bpy)_2dpp]^{2+}$ on 5′-GMP was strongly dependent on the presence of SMWCNTs. The reaction equation is shown in Fig. 3. The redox of 5′-GMP on $[Ru(bpy)_2dpp]^{2+}$/SMWCNTs/Au/GCE made by a simple method of cyclic voltametric deposition and drop coating produces a highly reversible redox peak that is very sensitive to changes in 5′-GMP independent of other interfering substances. The activity of the catalytic oxidation reaction decreased with the reduction of $[Ru(bpy)_2dpp]Cl_2$ molecules, resulting in a significant decrease in the 5′-GMP oxidation peak current [28].

The immobilization method of gold nanoparticles affects the sensitivity and accuracy of the electrode in

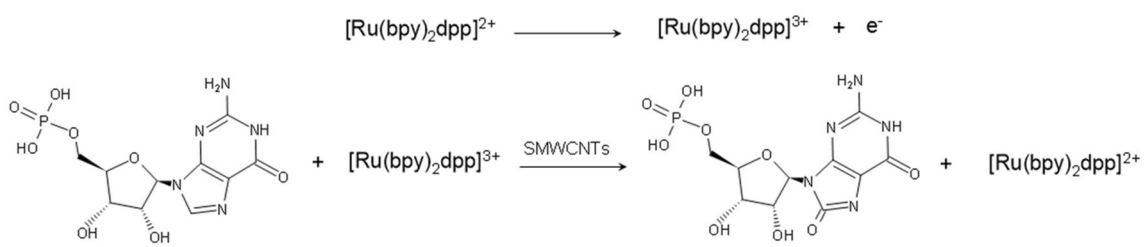

Fig. 3 The equation of the oxidation of $[Ru(bpy)_2dpp]^{2+}$ and 5′-GMP

the preparation of $[Ru(bpy)_2dpp]^{2+}$/SMWCNTs/Au/GCE. The loose connection between gold nanoparticles and bare GCE surface would directly lead to the decrease of sensor sensitivity. Two Au/GCEs obtained by two different immobilization methods (cyclic voltametric deposition and drop coating methods) were tested using electrochemical impedance spectroscopy method. The Nyquist diagram of the impedance spectra includes a semicircle part and a linear part, with the former at higher frequencies corresponding to the electron transfer limited process and the latter at lower frequencies corresponding to the diffusion process. The radius of the semicircle part is positively correlated with the resistance of the working electrode [29, 30]. The Nyquist plots of Au/GCE for the two immobilization methods of gold nanoparticles are shown in Fig. 4. The results show that the immobilization method of cyclic voltammetry deposition has the smallest impedance arc and the lowest resistance. This phenomenon implied that Au/GCE obtained by cyclic voltammetry deposition method has lower resistance, stronger electrical conductivity and higher sensitivity.

Optimization experiment

Optimization analysis of the pH of electrolyte

The pH of the electrolyte plays an important role in the proton transfer at the electrode-solution interface and can change the adsorption phenomenon and kinetics of charge transfer process on the electrode surface. Therefore, the effect of various PBS with pH ranging from 3 to 9 on the redox process of 5′-GMP (0.1 mmol L^{-1}) on $[Ru(bpy)_2dpp]^{2+}$/SMWCNTs/Au/GCE electrode was investigated. Disodium hydrogen phosphate and citric acid buffer solutions with 7 different pH values of 0.1 mmol/L 5′-GMP standard solution were used as the electrolyte for detection by cyclic voltammetry.

As shown in Fig. 5, the oxidation peak current of $[Ru(bpy)_2dpp]^{2+} \rightarrow [Ru(bpy)_2dpp]^{3+} + e^-$ remained constant with pH. On the contrary, the oxidation peak current of 5′-GMP decreased significantly with increasing pH, which was consistent with studies related to the greater susceptibility of 5′-GMP to oxidation under acidic conditions [31]. The oxidation peak current of 5′-GMP was maximum at pH 3, which is consistent with the choline monolayer carrier and gold nanocavity functionalized carbon nanotube sensing interface (pH 4) and carboxylated multi-walled carbon nanotubes/AuNPs modified glassy carbon electrode (pH 3) in comparison [32, 33].

Consequently, PBS at pH 3 was chosen as the most suitable electrolyte in this experiment to generate a larger response oxidation peak current of 5′-GMP.

Optimization analysis of the scan rate of CV

The effect of scan rate on the oxidation peak current of 5′-GMP was investigated to study the reaction kinetics of 5′-GMP on $[Ru(bpy)_2dpp]^{2+}$/SMWCNTs/Au/GCE. The CV curves of $[Ru(bpy)_2dpp]^{2+}$/SMWCNTs/Au/GCE in the 0.1 mmol L^{-1} 5′-GMP standard solution at pH = 3.0, with a preconditioning time of 300 s and scanning rates ranging from 20 to 260 mV s^{-1} are shown in Fig. 6. According to the figure, the oxidation peak current of 5′-GMP increased linearly with increasing

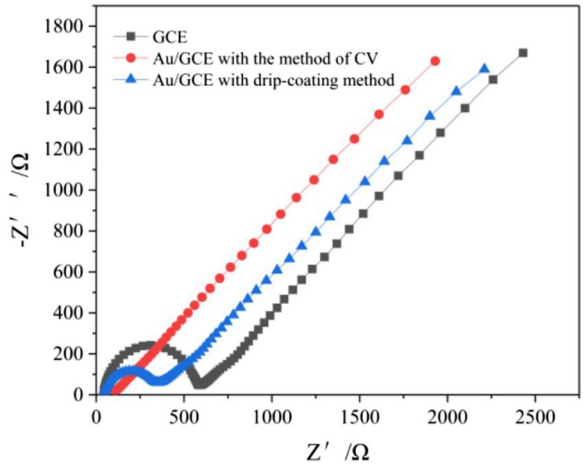

Fig. 4 The Nyquist plot of the impedance spectra of Au/GCE obtained by two different fixation methods (the methods of cyclic voltammetry deposition and drip-coating). Parameters: E_{init} = 0.255 V, high frequency = $1e^{+5}$ Hz, low frequency = 0.01 Hz, amplitude = 0.005 V

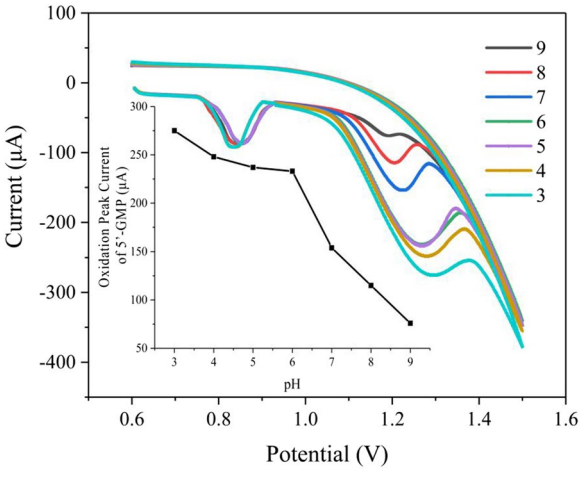

Fig. 5 CV curves of $[Ru(bpy)_2dpp]^{2+}$/SMWCNTs/Au/GCE in the solution of 0.1 mmol L^{-1} 5′-GMP with different pH (in the range of 3 to 9). Parameters: v = 100 mV s^{-1}, E_{range} = from 0.6 to 1.5 V, precondition potential = 0.6 V, precondition time = 300 s

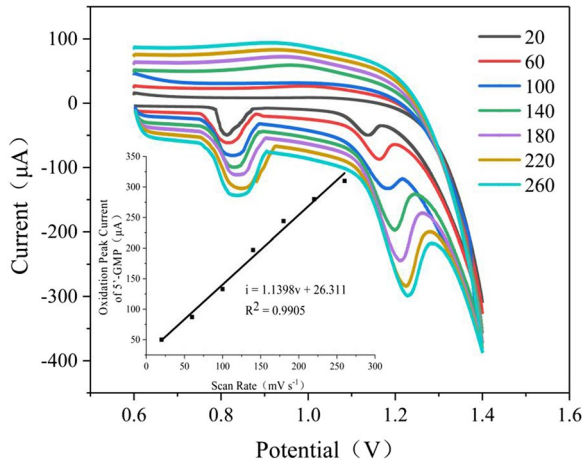

Fig. 6 CV curves of $[Ru(bpy)_2dpp]^{2+}$/SMWCNTs/Au/GCE in the solution of pH = 3 0.1 mmol L^{-1} 5′-GMP with different scan rate (in the range of 20 to 260 mV s^{-1}). Parameters: E_{range} = from 0.6 to 1.5 V, precondition potential = 0.6 V, precondition time = 300 s

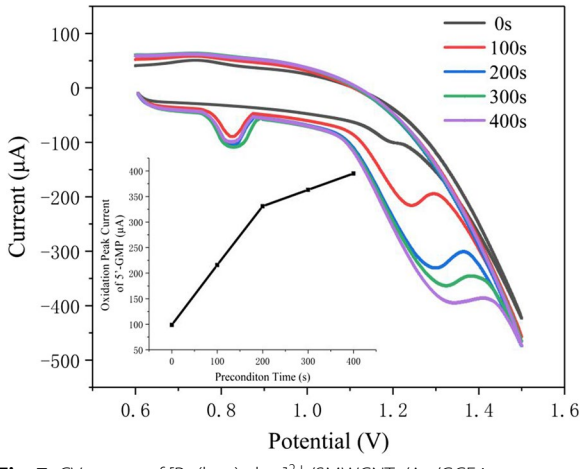

Fig. 7 CV curves of $[Ru(bpy)_2dpp]^{2+}$/SMWCNTs/Au/GCE in the solution of pH = 3 0.1 mmol L^{-1} 5′-GMP with different preconcentration time (in the range of 0 to 400 s). Parameters: v = 100 mV s^{-1}, E_{range} = from 0.6 to 1.5 V, *precondition potential* = 0.6 V

concentration at scan rate from 20 to 260 mV s^{-1} (i (μA) = 1.1398v (mV s^{-1}) + 26.311, R^2 = 0.9905). The results indicated that 5′-GMP and SMWCNT control the redox reaction mainly by adsorption under the catalytic effect of $[Ru(bpy)_2dpp]^{2+}$ [34]. The peak current shapes and values at each scan rate were compared with each other to clearly depict the CV curve of 5′-GMP oxidation at the electrode. A scan rate of 100 to 180 mV s^{-1} was chosen as the most appropriate scan rate. The peak current of 5′-GMP oxidation was weak when the scan rate was below 100 mV s^{-1}, but the peak current of oxidation was significantly shifted when the scan rate exceeded 180 mV s^{-1}.

Optimization analysis of the precondition time

The oxidation peak current of 5′-GMP was affected by the precondition time of 5′-GMP on $[Ru(bpy)_2dpp]^{2+}$/SMWCNTs/Au/GCE. Molecules of 5′-GMP accumulated on the electrode surface with sufficient pretreatment time but wasted time and too long precondition time wasted standard products [35]. Therefore, this experiment investigated the effect of pretreatment time of 5′-GMP on the response peak current using the CV method. The CV curves of $[Ru(bpy)_2dpp]^{2+}$/SMWCNTs/Au/GCE in 0.1 mmol L^{-1} 5′-GMP solution at pH = 3.0 with pretreatment time from 0 to 400 s and scan rate of 100 mV s^{-1} are shown in Fig. 7. When the pretreatment time was 0 s, the response current of $[Ru(bpy)_2dpp]^{2+}$ to $[Ru(bpy)_2dpp]^{3+}$ transition was 0 μA and the 5′-GMP oxidation response current was − 97.8 μA. The peak oxidation current of 5′-GMP was positively correlated with the precondition time, but when the precondition time was in the range of 300 to 400 s, the peak oxidation current grew slowly. This phenomenon may be due to the dense aggregation of particles in the electrolyte on the electrode surface, and the long pretreatment time would increase the resistance of the electrode. In conclusion, for the 5′-GMP assay, it is more appropriate to set the preconditioning time

Table 1 Reproducibility test of $[Ru(bpy)_2dpp]^{2+}$/SMWCNTs/Au/GCE in the solution of 0.1 mmol L^{-1} 5′-GMP

The sensor number	Number of detections						SD_2	CV_2 (%)
	1	2	3	4	5	6		
1	0.223	0.224	0.224	0.226	0.220	0.215	0.0036	1.62
2	0.225	0.225	0.226	0.225	0.220	0.214	0.0043	1.92
3	0.220	0.221	0.221	0.223	0.225	0.222	0.0016	0.74
SD_1	0.0021	0.0017	0.0021	0.0012	0.0024	0.0036		
CV_1(%)	0.9	0.7	0.9	0.6	1.0	1.6		

The values listed in the table were the peak current of the transition from $[Ru(bpy)_2dpp]^{3+}$ and 5′-GMP to $[Ru(bpy)_2dpp]^{2+}$ and 5′-GMP_{OX} with the unit of mA. SD_1 was the standard deviation within the group, SD_2 was the standard deviation between groups. CV_1 was the coefficient of variation within the group, and CV_2 was the coefficient of variation between the groups

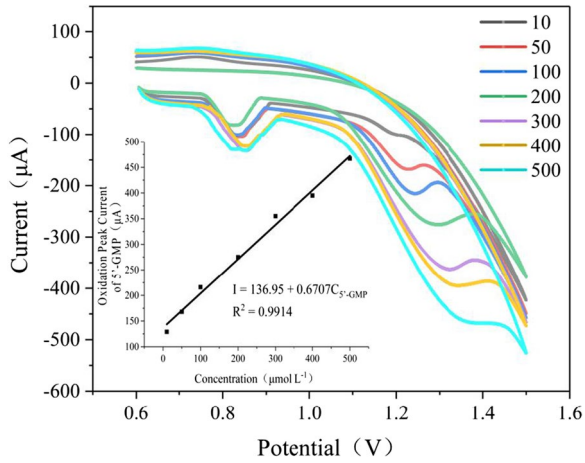

Fig. 8 CV curves of $[Ru(bpy)_2dpp]^{2+}$/SMWCNTs/Au/GCE in the solution of pH = 3 5′-GMP with different concentration (in the range of 0.01 to 0.5 mmol L^{-1}). Parameters: $v = 100$ mV s^{-1}, E_{range} = from 0.6 to 1.5 V, precondition potential = 0.6 V, precondition time = 300 s

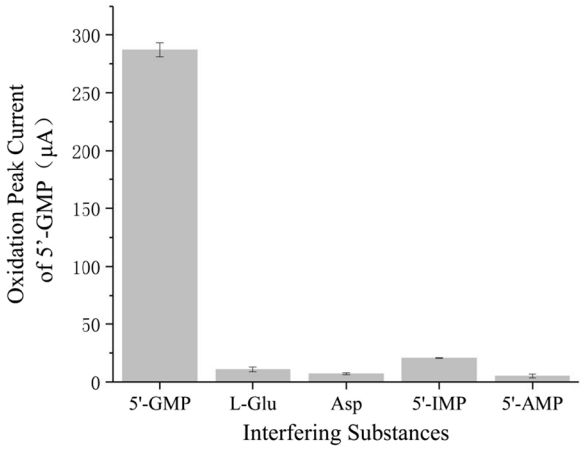

Fig. 9 Interference of $[Ru(bpy)_2dpp]^{2+}$/SMWCNTs/Au/GCE by L-Glu, Asp, 5′-IMP and 5′-AMP

to 300 s. The response current for the transition from $[Ru(bpy)_2dpp]^{2+}$ to $[Ru(bpy)_2dpp]^{3+}$ was about − 120 μA at a preconditioning time of 300 s. The response current for 5′-GMP oxidation also had a large value (− 387 μA) and a slight skew.

The linear range and detection limit of $[Ru(bpy)_2dpp]^{2+}$/SMWCNTs/Au/GCE

The detection performance of $[Ru(bpy)_2dpp]^{2+}$/SMWCNTs/Au/GCE for 5′-GMP was investigated under optimized conditions using the CV method. The inset in Fig. 8 highlights the linear response of the 5′-GMP oxidation peak current with respect to the 5′-GMP concentration. The linear equation was $y = 0.6707x + 136.95$, ($R^2 = 0.9914$), where "x" represented the concentration of 5′-GMP, and "y" represented the absolute value of the 5′-GMP oxidation peak current. 5′-GMP concentration could be determined by substituting the absolute value of peak current detected in the 5′-GMP solution with the unknown concentration into the linear equation above. The linear range was from 0.01 to 0.5 mmol L^{-1} and the detection limit was 0.0014 mmol L^{-1}.

The detection of selectivity

To investigate the selectivity of the $[Ru(bpy)_2dpp]^{2+}$/SMWCNTs/Au/GCE in more complex solution systems, interfering substances were selected according to 1) high levels of umami free amino acids in foods [36]. 2) substances with a structure similar to 5′-GMP [37, 38]. Therefore, we investigated the effects of some umami components, especially L-Glutamic acid (L-Glu), aspartic acid (Asp), inosine 5′-monophosphate (5′-IMP) and adenosine 5′-monophosphate (5′-AMP) as possible interfering compounds [39, 40]. Interfering substances such as L-Glu, Asp, 5′-IMP and 5′-AMP were added sequentially to 0.2 mmol L^{-1} 5′-GMP were added sequentially to 0.2 mmol L^{-1} 5′-GMP solution, and the changes of 5′-GMP oxidation peak currents are shown in Fig. 9. The rates of change of oxidation peak currents caused by L-Glu, Asp, 5′-IMP and 5′-AMP were 3.8%, 2.5%, 7.2% and 1.8%, respectively. The results showed that $[Ru(bpy)_2dpp]^{2+}$/SMWCNTs/Au/GCE had high selectivity and specificity for 5′-GMP, and interfering substances such as L-Glu, Asp, 5′-IMP and 5′-AMP had no effect on the determination of 5′-GMP.

The detection of reproducibility and stability

Reproducibility and stability are two important markers for measuring the performance of electrochemical sensors [41]. To investigate the reproducibility and stability of $[Ru(bpy)_2dpp]^{2+}$/SMWCNTs/Au/GCE, experiments were performed in a solution of 0.1 mmol/L 5′-GMP. Three bare GCE were modified with gold nanoparticles, $[Ru(bpy)_2dpp]^{2+}$ and SMWCNTs to make three

Table 2 The content of 5′-GMP in different cooking pots was detected by two methods ([Ru(bpy)2dpp]2 + /SMWCNTs/Au/GCE by electrode and HPLC method)

Cooking pots	HPLC (mg/100 g)	5′-GMP Sensor (mg/100 g)
1	1.16 ± 0.12	1.20 ± 0.08
2	1.48 ± 0.09	1.51 ± 0.08
3	1.91 ± 0.10	1.95 ± 0.06

Table 3 Performance comparison of $[Ru(bpy)_2dpp]^{2+}$/SMWCNTs/Au/GCE for 5′-GMP detection with other electrochemical sensors

Electrode	Modifier	Method	Linear dynamic range (μ M)	Detection limit (μ M)	Stability	References
GCE	Graphitic carbon nitride doped carboxylate MWCNTs nanocomposite	CV, DPV, EIS	0.18–36.32	0.040	–	[36]
GCE	Non-peripheral amine substituted nickel (II) phthalocyanine	CV, DPV	5–1000	5	–	[44]
GCE	Graphene and multi-walled carbon nanotubes	CV, EIS	0.1–59.7	0.025	After 2 weeks 94.69%	[45]
CILE	Ionic liquid 1-butyl-3-meth-ylimidazolium dihydrogen phosphate	CV, DPV, EIS	5–1000	1.3	After 1 month 92.2%	[46]
GCE	Graphene-Nafion	DPV	2–200	0.58	After 20 days 96.75%	[47]
GCE	$[Ru(bpy)_2dpp]^{2+}$/SMWCNTs/Au	CV, EIS	10–500	1.4	After 5 days 96.3%	Present work

$[Ru(bpy)_2dpp]^{2+}$/SMWCNTs/Au/GCE electrodes. Perform multiple CV tests on 0.1 mmol/L 5′-GMP, and the sensor should remain stable for 1 min after each data acquisition. Variations in the 5′-GMP oxidation peak current and relative standard deviation were recorded and calculated. Table 1 indicates that the value of CV_1 is between 0.6 and 1.6, and the value of CV_2 is in the range of 0.74 to 1.92, indicating that the measurement performance difference between the three 5′-GMP sensors is not obvious. Sensor 3 performed better than Sensors 1 and 2, and this difference might be due to differences in polish intensity of exposed GCE. The signal deviation of the 5′-GMP sensor was within 5 times of detection. Therefore, tests within 5 times could be used as a standard for one test. The cause of signal attenuation might be that $[Ru(bpy)_2dpp]Cl_2$ partially shed from GCE during repeated detection with a catalytic oxidation reaction.

$[Ru(bpy)_2dpp]^{2+}$/SMWCNTs/Au/GCE stability reference Nie's method with some modifications [42]. $[Ru(bpy)_2dpp]^{2+}$/SMWCNTs/Au/GCEs were placed at 4 ℃ for 15 d and detected at 5 d, 10 d and 15 d, respectively. Values of the oxidation peak current of 5′-GMP were 96.3%, 93.1%, 89.7% of the electrode just made respectively. The decrease in the peak oxidation current of 5′-GMP might be caused by the oxidation of $[Ru(bpy)_2dpp]^{2+}$ on the electrode surface [43]. Above results indicated that the good stability and reproducibility observed for the electrode of $[Ru(bpy)_2dpp]^{2+}$/SMWCNTs/Au/GCE used for the quantitative detection of 5′-GMP.

The detection of accuracy

Finally, in order to further prove the practicability and accuracy of present method, the 5′-GMP concentration detection of three different cooking pot sauce soups was calculated by using the developed $[Ru(bpy)_2dpp]^{2+}$/SMWCNTs/Au/GCE, and the calibration curve was obtained by using HPLC as a reference method. The results of these two methods are shown in Table 2. The 5′-GMP sensor determines the detection result values were well consistent with the data provided by HPLC. However, the results of 5′-GMP sensor were generally higher than those of HPLC. The reason for this deviation might be that $[Ru(bpy)_2dpp]^{2+}$ caused an oxidation reaction of part of the guanine or guanosine on the electrode surface in the broth, thereby increasing the response current. From the results above, the electrochemical modified sensor has the potential to effectively determine 5′-GMP in real samples. Comparison of the detection results with high performance liquid chromatography verified the practicality of the 5′-GMP electrochemical sensor. Table 3 brings together a comparison between several other electrochemical sensorsof 5'-GMP detection.

Abbreviations

5′-GMP: 5′-Guanylic acid; SMWCNTs: Sulfonated-multiwalled carbon nanotubes; GCE: Glass carbon electrode; CV: Cyclic voltammetry; EIS: Electrochemical impedance spectroscopy; DMF: N, N-Dimethylformamide; L-Glu: L-Glutamic acid; Asp: Aspartic acid; 5′-IMP: Inosine 5′-monophosphate; 5′-AMP: Adenosine 5′-monophosphate; PBS: Phosphate buffer solutions; HPLC: High-performance liquid chromatograph.

Acknowledgements

The authors thank the support of this work by Bohai University and Jilin University, and this work was supported by the Natural Science Foundation of Liaoning province [Grant Number 2019-MS-006].

Author contributions

YY analyzed the data and writing-reviewed and edited, SH performed the experiments, XW and DL conceived and designed the experiments, CY performed a grammar check. All authors read and approved the final manuscript.

Funding

Natural Science Foundation of Liaoning Province, 2019-MS-006, Dengyong Liu.

Availability of data and materials

The datasets generated during and/or analyzed during the current study are available from the corresponding authors on reasonable request.

Declarations

Competing interests
The authors declare that they have no competing interests.

Author details
[1]National and Local Joint Engineering Research Center of Storage,, Processing and Safety Control Technology for Fresh Agricultural and Aquatic Products, College of Food Science and Technology, Bohai University, Jinzhou 121013, China. [2]Jiangsu Collaborative Innovation Center of Meat Production and Processing, Quality and Safety Control, Nanjing 210095, China. [3]College of Food Science and Engineering, Jilin University, Changchun 130062, China.

Received: 24 March 2022 Accepted: 19 July 2022
Published online: 03 August 2022

References
1. Rotola-Pukkila M, Yang BR, Hopia A (2019) The effect of cooking on umami compounds in wild and cultivated mushrooms. Food Chem 278(25):56–66. https://doi.org/10.1016/j.foodchem.2018.11.044
2. Rocha RAR, Ribeiro MN, Silva GA, Rocha LCR, Piheiro ACM, Nunes CA, Carneiro JDS (2020) Temporal profile of flavor enhancers MAG, MSG, GMP, and IMP, and their ability to enhance salty taste, in different reductions of sodium chloride. J Food Sci 85(5):1565–1575. https://doi.org/10.1111/1750-3841.15121
3. Huang YL, Lu DQ, Liu H, Liu SY, Jiang S, Pang GC, Liu Y (2019) Preliminary research on receptor-ligand recognition mechanism of umami by hT1R1 biosensor. Food Funct 10(3):1280–1287. https://doi.org/10.1039/C8FO02522C
4. Chen Q, Mou S, Hou X (1999) Determination of inosine 5′-monophosphate and guanosine 5′-monophosphate in taste-enhancers by ion chromatography. Se pu Chin J Chromatogr/Zhongguo hua xue hui 17:290–292
5. Domínguez-álvarez J, Mateos-Vivas M, Rodríguez-Gonzalo E, García-Gómez D, Bustamante-Rangel M, Zamarreno MMD, Carabias-Martínez R (2017) Determination of nucleosides and nucleotides in food samples by using liquid chromatography and capillary electrophoresis. TrAC, Trends Anal Chem 92(3):12–31. https://doi.org/10.1016/j.trac.2017.04.005
6. Dai LZ, Guo N, Liu YQ, Shen SS, Ge QF, Pan YJ (2019) Analysis of the binding sites with NL-101 to amino acids and peptides by HPLC/MS/MS. Chin Chem Lett 30(1):103–106. https://doi.org/10.1016/j.cclet.2017.12.023
7. Xu Y, Kutsanedzie FYH, Hassan MM, Zhu JJ, Ahmad W, Li HH, Chen QS (2020) Mesoporous silica supported orderly-spaced gold nanoparticles SERS-based sensor for pesticides detection in food. Food Chem 315:126–300. https://doi.org/10.1016/j.foodchem.2020.126300
8. Li WL, Yao L, Zhang ZW, Geng HC, Li CC, Yu YY, Sheng PT, Li ST (2019) Tiny Au nanoparticles mediation strategy for preparation of NIR CuInS2 QDs based 1D TiO_2 hybrid photoelectrode with enhanced photocatalytic activity. Mater Sci Semicond Process 99:106–113. https://doi.org/10.1016/j.mssp.2019.04.021
9. Rasheed T, Bilal M, Nabeel F, Lqbal HMN, Li CL, Zhou YF (2018) Fluorescent sensor-based models for the detection of environmentally related toxic heavy metals. Sci Total Environ 615(1):476–485. https://doi.org/10.1016/j.scitotenv.2017.09.126
10. Dang YL, Hao L, Zhou TY, Cao JX, Sun YY, Pan DD (2019) Establishment of new assessment method for the synergistic effect between umami peptides and monosodium glutamate using electronic tongue. Food Res Int 121:20–27. https://doi.org/10.1016/j.foodres.2019.03.001
11. Westhuizen DVD, Eschwege KGVJ, Conradie J (2019) Electrochemistry and spectroscopy of substituted $[Ru(phen)_3]^{2+}$ and $[Ru(bpy)_3]^{2+}$ complexes. Electrochemical Acta 320:134540–134540. https://doi.org/10.1016/j.electacta.2019.07.051
12. Chen YM, Liu YJ, Li Q, Wang KZ (2009) pH- and DNA-induced dual molecular light switches based on a novel ruthenium (II) complex. J Inorg Biochem 103(10):1395–1404. https://doi.org/10.1016/j.jinorgbio.2009.08.002
13. Hall JP, Gurung SP, Henle J, Poidl P, Andersson DJ, Lincoln DP, Winter G, Sorensen T, Cardin PDJ, Brazier DJA, Cardin PCJ (2017) Guanine can direct binding specificity of Ru-dipyridophenazine (dppz) complexes to DNA through steric effects. Chem Eur J 23(21):4981–4985. https://doi.org/10.1002/chem.201605508
14. Xie H, Yang D, Heller A, Gao ZQ (2007) Electrocatalytic oxidation of guanine, guanosine, and guanosine monophosphate. Biophys J 92(8):L70–L72. https://doi.org/10.1529/biophysj.106.102632
15. Chen MJ, Weng XM, Qing LY, Xu SD, Li H (2011) Electrocatalytic activity of $[Ru(bpy)_3]^{2+}$, toward guanine oxidation upon incorporation of surfactants and SWCNTs. J Appl Electrochem 41(7):795–801. https://doi.org/10.1007/s10800-011-0297-9
16. Stemp EDA, Arkin MR, Barton JK (1997) Oxidation of guanine in DNA by $Ru(phen)_2(dppz)^{3+}$ using the Flash-Quench technique. J Am Chem Soc 119(12):2921–2925. https://doi.org/10.1021/ja963606p
17. Wu ZY, Zhang QX, Huang LJ, Xu YJ, Tang DL (2021) Covalent immobilization of ruthenium polypyridyl complex on multi-walled carbon nanotube supports for oxygen evolution reaction in an alkaline solution. J Power Sources 488:229448. https://doi.org/10.1016/j.jpowsour.2020.229448
18. Setznagl S, Cesarino I (2020) Copper nanoparticles and reduced graphene oxide modified a glassy carbon electrode for the determination of glyphosate in water samples. Int J Environ Anal Chem. https://doi.org/10.1080/03067319.2020.1720667
19. Li G, Zhao XX, Wang L, Liu WS (2019) Chiral zinc complexes used as fluorescent sensor for natural amino acids. Chem Select 4(32):9317–9321. https://doi.org/10.1002/slct.201902139
20. Bhuiyan AA, Kincaid JR (1999) Synthesis and spectroscopic characterization of a zeolite-entrapped $Ru(bpy)_2(dpp)^{2+}$ complex. Inorg Chem 38(21):4759–4764. https://doi.org/10.1021/ic990359s
21. Subagio A, Taufiq HR, Khumaeni A, Umiati NA, Adi K (2022) Simple method for making MWCNTs/Au-NPs-based biosensor electrodes. Mater Res Express. https://doi.org/10.1088/2053-1591/ac4b75
22. Yoo LH, Kim H (2011) Conductivities of graphite fiber composites with single-walled carbon nanotube layers. Int J Precis Eng Manuf 12:745–748. https://doi.org/10.1007/S12541-011-0098-4
23. Duc Chinh V, Speranza G, Migliaresi C, Van Chuc N, Minh Tan V, Phuong N (2019) Synthesis of gold nanoparticles decorated with multiwalled carbon nanotubes (Au-MWCNTs) via cysteaminium chloride functionalization. Sci Rep. https://doi.org/10.1038/s41598-019-42055-7
24. Neeley WL, Essigmann J (2006) Mechanisms of formation, genotoxicity, and mutation of guanine oxidation products. Chem Res Toxicol 19(4):491–505. https://doi.org/10.1021/tx0600043
25. Tanik NA, Demirkan E, Avkut Y (2018) Guanine oxidation signal enhancement in DNA via a polyacrylonitrile nanofiber-coated and cyclic voltammetry-treated pencil graphite electrode. J Phys Chem Solids 118:73–79. https://doi.org/10.1016/j.jpcs.2018.03.001
26. Brett AMO, Diculescu V, Piedade JAP (2002) Electrochemical oxidation mechanism of guanine and adenine using a glassy carbon microelectrode. Bioelectrochemistry 55(1–2):61–62. https://doi.org/10.1016/S1567-5394(01)00147-5
27. Hong W, Li H, Yao S, Sun F, Xu ZH (2009) Mediated oxidation of guanine by $[Ru(bpy)_2d\ pp]^{2}+$ and their electrochemical assembly on the ITO electrode. Electrochem Acta 54(12):3250–3254. https://doi.org/10.1016/j.electacta.2008.12.031
28. Wang QL, Chen MM, Zhang HQ, Wen W, Zhang XH, Wang SF (2016) Solid-state electrochemiluminescence sensor based on RuSi nanoparticles combined with molecularly imprinted polymer for the determination of ochratoxin A. Sens Actuators, B Chem 222:264–269. https://doi.org/10.1016/j.snb.2015.08.057
29. Wünsche M, Schillinger C, Mitterbach A, Geis-Gerstorfer J, Prokop G (2019) Electrochemical impedance spectroscopy and corrosion point counting on metal sheet edges with different cathodic dip coat materials. Mater Corros 70(6):1026–1035. https://doi.org/10.1002/maco.201810392
30. Shaffer DL, Feldman KE, Chan EP, Stafford GR, Stafford CM (2019) Characterizing salt permeability in polyamide desalination membranes using electrochemical impedance spectroscopy. J Membr Sci 583:248–257. https://doi.org/10.1016/j.memsci.2019.04.062
31. Liska A, Triskova L, Ludvik J, Trnkova L (2019) Oxidation potentials of guanine, guanosine and guanosine-5′-monophosphate: theory and experiment. Electrochem Acta 318:108–119. https://doi.org/10.1016/j.electacta.2019.06.052

32. Feng QM, Wang MY, Chen Q, Wang P (2018) Direct electrochemical detection of guanosine-5′-monophosphate at choline monolayer supported and gold nanocages functionalized carbon nanotubes sensing interface. Sens Actuators, B Chem 274:343–348. https://doi.org/10.1016/j.snb.2018.07.114
33. Wang J, Zhu LY, Zhang WL, Wei ZB (2019) Application of the voltametric electronic tongue based on nanocomposite modified electrodes for identifying rice wines of different geographical origins. Anal Chem Acta 1050:60–70. https://doi.org/10.1016/j.aca.2018.11.016
34. Choi SJ, Lee DM, Yu H, Jang JS, Kim MH, Kang JY, Jeong HS, Kim HD (2019) All-carbon fiber-based chemical sensor: Improved reversible NO2 reaction kinetics. Sens Actuators, B Chem 290:293–301. https://doi.org/10.1016/j.snb.2019.03.134
35. Shetti NP, Malode SJ, Llager D, Kakarla RR, Shukla SS, Aminabhavi TM (2019) A novel electrochemical sensor for detection of molinate using ZnO nanoparticles loaded carbon electrode. Electroanalysis 31(6):163–173. https://doi.org/10.1002/elan.201800775
36. Fei QQ, Zhang NN, Sun C, Zhang PP, Yang XD, Hua YH, Li L (2019) A novel non-enzymatic sensing platform for determination of 5′-guanosine monophosphate in meat. Food Chem 286:515–521. https://doi.org/10.1016/j.foodchem.2019.02.052
37. Pagliara AS, Goodman AD (1970) Effect of 3′,5′-GMP and 3′,5′-IMP on production of glucose and ammonia by renal cortex. Am J Physiol 218(5):1301–1306. https://doi.org/10.1152/ajplegacy.1970.218.5.1301
38. Phan CW, Wang JK, Cheah SC, Naidu M, David P, Sabaratnam V (2017) A review on the nucleic acid constituents in mushrooms: nucleobases, nucleosides and nucleotides. Crit Rev Biotechnol 38(5):762–777. https://doi.org/10.1080/07388551.2017.1399102
39. Kong Y, Yang X, Ding Q, Zhang YY, Sun BG, Chen HT, Sun Y (2017) Comparison of non-volatile umami components in chicken soup and chicken enzymatic hydrolysate. Food Res Int 102:559–566. https://doi.org/10.1016/j.foodres.2017.09.038
40. Sun C, Gao L, Wang DY, Zhang MH, Liu Y, Geng ZM, Xu WM, Liu F, Bian H (2016) Biocompatible polypyrrole-block copolymer-gold nanoparticles platform for determination of inosine monophosphate with bi-enzyme biosensor. Sens Actuators, B Chem 230:521–527. https://doi.org/10.1016/j.snb.2016.02.111
41. Zhang C, Chen XH, Tan LJ, Wang JT (2018) Combined toxicities of copper nanoparticles with carbon nanotubes on marine microalgae Skeletonema costatum. Environ Sci Pollut Res 25(13):13127–131331. https://doi.org/10.1007/s11356-018-1580-7
42. Nie Q, Zhang W, Wang LR, Guo Z, Li CY, Yao J, Li M, Wu DM, Zhou LQ (2018) Sensitivity enhanced stability improved ethanol gas sensor based on multi-wall carbon nanotubes functionalized with Pt-Pd nanoparticles. Sens Actuators B Chem 270(1):140–148. https://doi.org/10.1016/j.snb.2018.04.170
43. Yu LY, Zhang Q, Yang BR, Xu Q, Xu Q, Hu XY (2018) Electrochemical sensor construction based on Nafion/calcium lignosulphonate functionalized porous graphene nanocomposite and its application for simultaneous detection of trace Pb^{2+} and Cd^{2+}. Sens Actuators, B Chem 259:540–551. https://doi.org/10.1016/j.snb.2017.12.103
44. Jeevagan A, John S (2013) Electrochemical determination of guanosine 5′-monophosphate using the electropolymerized film of non-peripheral amine substituted nickel (II) phthalocyanine modified electrode. Electrochem Acta 95:246–250. https://doi.org/10.1016/j.electacta.2013.02.025
45. Yin H, Zhou Y, Ma Q, Liu T, Ai S, Zhu L (2010) Electrochemical oxidation behavior of guanosine-5′-monophosphate on a glassy carbon electrode modified with a composite film of graphene and multi-walled carbon nanotubes, and its amperometric determination. Microchem Acta 172(3–4):343–349. https://doi.org/10.1007/s00604-010-0499-6
46. Shi F, Wang X, Wang W, Sun W (2015) Electrochemical behavior and determination of guanosine-5′-monophosphate on a ionic liquid modified carbon electrode. J Anal Chem 70(2):186–192. https://doi.org/10.1134/s1061934815020057
47. Yin H, Zhou Y, Ma Q, Ai S, Ju P, Zhu L, Lu L (2010) Electrochemical oxidation behavior of guanine and adenine on graphene–Nafion composite film modified glassy carbon electrode and the simultaneous determination. Process Biochem 45(10):1707–1712. https://doi.org/10.1016/j.procbio.2010.07.004

Publisher's Note